

# Complexation and Molecular Speciation in the Silica Sol–Gel Process Characterized by Electrospray Ionization Fourier Transform Ion-Cyclotron Resonance Mass Spectrometry

Robert E. Bossio,<sup>†,‡</sup> Sean D. Callahan,<sup>†</sup> Albert E. Stiegman,<sup>\*,†</sup> and Alan G. Marshall<sup>\*,†,‡</sup>

Department of Chemistry, Florida State University, Tallahassee, Florida 32306, and Center for Interdisciplinary Magnetic Resonance, The National High Magnetic Field Laboratory, 1800 East Paul Dirac Drive, Tallahassee, Florida 32310

Received December 11, 2000. Revised Manuscript Received March 26, 2001

The sol–gel reactions of tetraethyl orthosilicate have previously been characterized by various instrumental methods, each revealing different aspects of the reactions that eventually form glass, SiO<sub>2</sub>. In this paper, we use electrospray ionization Fourier transform ion-cyclotron resonance mass spectrometry (ESI FT-ICR MS) to characterize the hydrolysis and condensation intermediates based on alkali and transition metal ion attachment to ionize the intermediates. Sodium trifluoromethanesulfonate and nickel(II) nitrate hexahydrate were added to solutions containing tetraethyl orthosilicate, electrosprayed, and the resulting species observed. Sodium ion binds nonspecifically to silicates, whereas nickel produces a tris-tetraethyl orthosilicate nickel(II) complex. Sodium-bound dimers were also observed; they could be dissociated without damage to the silicate backbone by infrared multiphoton dissociation. It is thus possible to observe all of the hydrolysis products (OH exchanged for OCH<sub>2</sub>CH<sub>3</sub>) for a given silicate oligomer as well as different silicate oligomers.

## Introduction

Because of its general technological importance, most stages of the sol–gel process for the production of pure and multicomponent amorphous silica materials have been well investigated.<sup>1</sup> In particular, the early solution phase of the process has generated a number of excellent studies aimed at elucidating the kinetics and mechanism of the reaction.<sup>2–6</sup> Investigations of both the acid- and base-catalyzed pure silica sol–gel reactions have identified a variety of small linear, branched, and cyclic polysilicates in the early stages of the reaction.<sup>7–12</sup>

These studies have ultimately related reaction conditions to the properties of the final xerogel.<sup>13–15</sup>

Common approaches to elucidating species in solution have been <sup>29</sup>Si NMR and gas chromatography electron-ionization mass spectroscopy (GC EI-MS). Although these methods have positively identified a number of silicate species, they are generally limited to the initial stages of the process or to reactions carried out with substoichiometric amounts of water. In particular, <sup>29</sup>Si NMR does not provide structural information, except during the early stages of the reaction, beyond the relative distribution of silicons in particular coordination environments, whereas GC EI-MS is restricted to volatile silicates, thereby limiting the observed species to relatively low molecular weights and limited degrees of hydrolysis.

Recently, chemical ionization mass spectrometry has been applied to the characterization of species formed in the sol–gel synthesis of polysilsesquioxanes.<sup>16</sup> Unlike GC EI-MS, this soft ionization technique can generate intact molecular species for more direct characterization of reacting species. Further improvements in volatilization, ionization, mass resolution, and mass accuracy promise to provide even more information about mo-

\* To whom correspondence should be addressed.

<sup>†</sup> Florida State University.

<sup>‡</sup> The National High Magnetic Field Laboratory.

(1) Brinker, C. J.; Scherer, G. W. *Sol Gel Science*, 1st ed.; Academic Press: Boston, 1990; Vol. 1.

(2) Assink, R. A.; Kay, B. D. *J. Non-Cryst. Solids* **1988**, *99*, 359–370.

(3) Kay, B. D.; Assink, R. A. *J. Non-Cryst. Solids* **1988**, *104*, 112–122.

(4) Pouxviel, J. C.; Boilot, J. P. *J. Non-Cryst. Solids* **1987**, *94*, 374–386.

(5) Ro, J. C.; Chung, I. J. *J. Non-Cryst. Solids* **1989**, *110*, 26–32.

(6) Sanchez, J.; McCormick, A. V. *J. Phys. Chem.* **1992**, *96*, 8973–8979.

(7) Klemperer, W. G.; Mainz, V. V.; Ramamurthi, S. D., Eds.; Materials Research Society: Pittsburgh, PA, 1988; p 15.

(8) Klemperer, W. G.; Ramamurthi, S. D., Ed.; Materials Research Society: Pittsburgh, PA, 1988; p 1.

(9) Brunet, F.; Cabane, B. *J. Non-Cryst. Solids* **1993**, *211*–225.

(10) Ng, L. V.; McCormick, A. V. *J. Phys. Chem.* **1996**, *100*, 12517–12531.

(11) Badescu, V.; Zaharescu, M.; Vasilescu, A.; Radu, M. *Rev. Roum. Chim.* **1996**, *41*, 733–740.

(12) Zaharescu, M.; Badescu, V.; Vasilescu, A.; Radu, M. *Rev. Roum. Chim.* **1997**, *42*, 633–639.

(13) Brinker, C. J.; Keefer, K. D.; Schaefer, D. W.; Ashley, C. S. *J. Non-Cryst. Solids* **1982**, *48–64*, 47.

(14) Brinker, C. J.; Keefer, K. D.; Schaefer, D. W.; Assink, R. A.; Kay, B. D.; Ashley, C. S. *J. Non-Cryst. Solids* **1984**, *63*, 45–59.

(15) Brinker, C. J.; Scherer, G. W. *J. Non-Cryst. Solids* **1985**, *70*, 301–322.

(16) Loy, D. A.; Beach, J. V.; Baugher, B. M.; Assink, R. A.; Shea, K. J.; Tran, J.; Small, J. H. *Chem. Mater.* **1999**, *11*, 3333–3341.

lecular speciation under specific conditions and molecular growth pathways as a function of time.

Here, we report the first successful application of electrospray ionization Fourier transform ion-cyclotron resonance mass spectrometry (ESI FT-ICR MS) to the elucidation of complex molecular species in the silicon alkoxide sol-gel process. Electrospray ionization is capable of generating and transporting high molecular weight species into the gas phase, as demonstrated previously for numerous biological molecules and some inorganic polymers.<sup>17-21</sup> In addition, when ions are present in solution, ESI can deliver them intact to the gas phase. Unlike gas-chromatography-based techniques, ESI is not limited by volatility and can transport potentially all of the polar species from a complex mixture into the gas phase, thereby giving a picture of those species present in solution. When ESI is combined with FT-ICR MS, which affords the highest possible mass resolving power and mass accuracy, complex mixtures can be analyzed with great success.<sup>22,23</sup>

### Experimental Section

Tetraethyl orthosilicate (99.995%), lithium, sodium, potassium trifluoromethane sulfonate ("triflate") (98%), and glacial acetic acid were obtained from Aldrich Chemical Co. (Milwaukee, WI). Nickel sulfate hexahydrate (99+%) was purchased from Sigma. Methanol, acetonitrile (Burdick and Jackson, 99.9% HPLC grade), and water (99.9% Fischer HPLC grade) were obtained from Fischer Scientific. All chemicals were used without further purification.

Each of the alkoxy silicates was electrosprayed from a 1:1 mole ratio mixture of water/acetonitrile. The sol-gel solutions were 1.36 M in TEOS with a 3:1 H<sub>2</sub>O:TEOS ratio with ethanol as a cosolvent. Just prior to analysis the solution was diluted to 300  $\mu$ M for electrospraying. For the samples containing an alkali trifluoromethane sulfonate, the salt was added to give a final concentration of 10  $\mu$ M. For experiments involving nickel(II) ions, nickel(II) sulfate was added to 300  $\mu$ M tetraethyl orthosilicate in dry acetonitrile to yield a final Ni(II) concentration of 10  $\mu$ M.

Electrospray FT-ICR mass spectra were produced with a home-built 9.4-T instrument equipped with a modular ICR data station, both described in detail elsewhere.<sup>24,25</sup> Electrospray ionization was performed at a solution flow rate of 0.2  $\mu$ L/min, emitter potential of 3 kV, and skimmer potential of 350 V. Ions were accumulated in an external octapole (1.5 MHz, 166 V<sub>p-p</sub> rf, and 70 V dc) for 10 s before transfer to the ICR cell.<sup>26</sup> One mass spectrum was collected per sample, with the octapole ion guide operated at 1.7 MHz, allowing transmission of ions over a mass-to-charge ratio range of  $200 \leq m/z \leq 2000$ .

Each 2-MB time-domain transient was the sum of 36 coadded transients. The transients were zero-filled once, Hamming-apodized, Fourier-transformed, converted to magnitude mode, and subjected to standard frequency-to- $m/z$  conversion.<sup>27,28</sup> For mass calibration, angiotensin II (monoisotopic exact mass 1044.5505) was added to concentration of 10  $\mu$ M to a partially hydrolyzed solution of TMOS in 1:1 water:methanol, and then brought to 10  $\mu$ M in sodium triflate. A time-domain signal consisting of 36 coadded transients was Fourier transformed, Hamming apodized, and converted from frequency to  $m/z$ .<sup>27,28</sup> Internal mass calibration was based on the M, M + 1, and M + 2 peaks for the +2 and +3 charge states of angiotensin. It was then possible to identify various TMOS and hydrolysis product species to within 1 ppm rms deviation between experimental mass and the mass computed from elemental composition. The TMOS and hydrolysis product species then served as internal calibrants for the remaining mass spectra. Elemental composition assignments were based on matching experimental  $m/z$  values to those computed from Isopro 3.1 for possible silicate structures.<sup>29</sup> Agreement between theoretical and experimental  $m/z$  values was typically closer than 10 ppm (prior to internal calibration) for all of the systems studied.

Infrared multiphoton dissociation (IRMPD)<sup>30-32</sup> mass spectra were obtained by stored-waveform inverse Fourier transform (SWIFT<sup>33,34</sup>) isolation of the parent ion, followed by irradiation with a CO<sub>2</sub> laser (10.6- $\mu$ m wavelength) at 4 W for 750 ms. Time-domain transients were collected and processed as above.

### Results and Discussion

**Silicate-Alkali Metal Complexation.** McCormick et al. have shown by <sup>29</sup>Si NMR that alkali metal cations interact with anionic silicate fragments (SiO<sup>-</sup>) in aqueous or alcoholic media, thereby promoting condensation of the silica.<sup>35</sup> We have determined that nonionic complexation between neutral silicates species and metal cations is sufficiently strong that the association complexes may be put into the gas phase in concentrations suitable for mass spectral analysis by electrospray ionization. Figure 1 shows an ESI FT-ICR mass spectrum of tetraethyl orthosilicate (TEOS) (300  $\mu$ M) in an acetonitrile solution containing sodium triflate (10  $\mu$ M). Clearly identifiable as singly charged ions of 365.1423  $\pm$  0.0004 and 439.2152  $\pm$  0.0005 Da are the sodiated monomer, [(TEOS)Na]<sup>+</sup>, and the sodium-bound dimer (see below), [(TEOS)Na(TEOS)]<sup>+</sup>. (Multiply charged ions are ruled out by the absence of nuclides containing one <sup>13</sup>C or <sup>29</sup>Si at integral fractions of 1 Da above the mass of the monoisotopic species (e.g., all carbons are <sup>12</sup>C; all silicons are <sup>28</sup>Si; all oxygens are <sup>16</sup>O). Although electrospray ionization of alkali metal adducts is well-known for other systems (e.g., poly(ethylene)glycol), the formation of such adducts with neutral silicon alkoxides and

(17) Fenn, J. B.; Mann, M.; Meng, C. K.; Wong, S. F.; Whitehouse, C. M. *J. Am. Soc. Mass Spectrom.* **1989**, *64*-71.

(18) Yamashita, S. F.; Meng, C. K.; Fenn, J. B. *J. Phys. Chem.* **1988**, *92*, 546-50.

(19) Andersen, U.; König, S.; Leary, J. A.; Freitas, M. A.; Marshall, A. G. *J. Am. Soc. Mass Spectrom.* **1999**, *10*, 352-354.

(20) Colton, R.; D'Agostino, A.; Traeger, J. C. *Mass Spectrom. Rev.* **1995**, *14*, 79-106.

(21) Kriesel, J. W.; König, S.; Freitas, M. A.; Marshall, A. G.; Leary, J. A.; Tilley, T. D. *J. Am. Chem. Soc.* **1998**, *120*, 12207-12215.

(22) Marshall, A. G.; Hendrickson, C. L.; Emmett, M. R. *Recent Advances in Fourier Transform Ion Cyclotron Resonance Mass Spectrometry*; Marshall, A. G., Hendrickson, C. L., Emmett, M. R., Eds.; Elsevier: Amsterdam, 1998; Vol. 14, pp 219-237.

(23) Rodgers, R. P.; Blumer, E. N.; Freitas, M. A.; Marshall, A. G. *Anal. Chem.* **1999**, *71*, 5171-5176.

(24) Senko, M. W.; Hendrickson, C. L.; Pasa-Tolic, L.; Marto, J. A.; White, F. M.; Guan, S.; Marshall, A. G. *Rapid Commun. Mass Spectrom.* **1996**, *10*, 1824-1828.

(25) Senko, M. W.; Canterbury, J. D.; Guan, S.; Marshall, A. G. *Rapid Commun. Mass Spectrom.* **1996**, *10*, 1839-1844.

(26) Senko, M. W.; Hendrickson, C. L.; Emmett, M. R.; Shi, S. D.-H.; Marshall, A. G. *J. Am. Soc. Mass Spectrom.* **1997**, *8*, 970-976.

(27) Ledford, E. B., Jr.; Rempel, D. L.; Gross, M. L. *Anal. Chem.* **1984**, *56*, 2744-2748.

(28) Shi, S. D.-H.; Drader, J. J.; Freitas, M. A.; Hendrickson, C. L.; Marshall, A. G. *Int. J. Mass Spectrom.* **2000**, *195/196*, 591-598.

(29) Senko, M. W. *IsoPro version 3.1* (<http://members.aol.com/msmssoft>); Senko, M. W., Ed., 1998.

(30) Woodlin, R. L.; Bomse, D. S.; Beauchamp, J. L. *J. Am. Chem. Soc.* **1978**, *100*, 3248-3250.

(31) Watson, C. H.; Baykut, G.; Eyley, J. R. *ACS Symp. Ser.* **1987**, *359*, 140-154.

(32) Little, D. P.; Speir, J. P.; Senko, M. W.; O'Connor, P. B.; McLafferty, F. W. *Anal. Chem.* **1994**, *66*, 2809-2815.

(33) Marshall, A. G.; Wang, T.-C. L.; Ricca, T. L. *J. Am. Chem. Soc.* **1985**, *107*, 7893-7897.

(34) Guan, S.; Marshall, A. G. *Int. J. Mass Spectrom. Ion Process.* **1996**, *157/158*, 5-37.

(35) McCormick, A.; Sanchez, J. *Chem. Mater.* **1991**, *3*, 320-324.

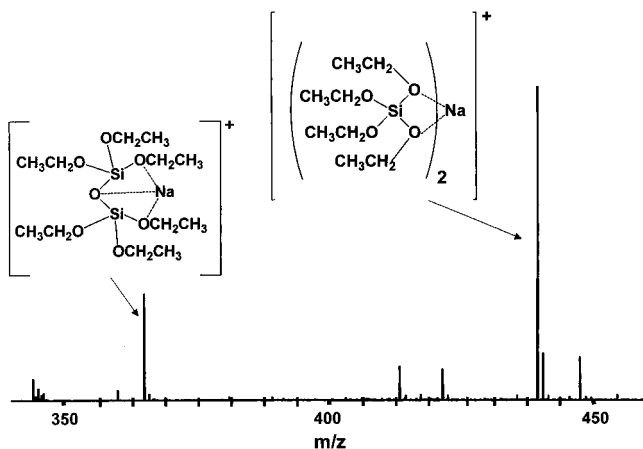


**Figure 1.** ESI FT-ICR positive-ion mass spectrum showing the two ion types observed for alkoxy-silicates. The sodium ion adduct at 439.2152 Da is a sodium-bound dimer of two TEOS monomers. The peak at 365.1423 Da arises from sodium bound to a silicate dimer.

in the acid-catalyzed alcoholic sol-gel reaction of these alkoxides has not been observed previously.<sup>18</sup>

For the alkali-metal silica sol-gel system, the binding preference of the alkali-metal adducts with  $\text{SiO}^-$  has previously been observed to follow the trend  $\text{Li}^+ < \text{Na}^+ < \text{Cs}^+ < \text{Rb}^+ < \text{K}^+$ .<sup>6,36</sup> That rank order was interpreted as arising from a balance between the solvation of the cation and the strength of the ion pair. ESI FT-ICR mass spectral relative abundances rank as  $\text{Li}^+:\text{Na}^+:\text{K}^+ = 9:6:4$ . If the electrospray ionization efficiencies are comparable, then those relative abundances would reflect binding preferences of the alkali metal for TEOS in solution. If so, the observed rank order is the reverse of that found for  $\text{SiO}^-$  interactions in solution. Since there can be no ion-pair bond ( $\text{Si}-\text{O}^- \cdots \text{M}^+$ ) between the metal ion and the peralkylated silicate, adduct formation would be expected to depend only on the solvation energy of the ion. Ion solvation energies (alkali cations in water) follow the order  $\text{Li}^+ > \text{Na}^+ > \text{K}^+$ , consistent with the observed ESI FT-ICR MS ion relative abundance trend.<sup>36</sup> Notably, direct electrospray of protonated silicates (as would naturally be present in acid-catalyzed solutions) yields few gas-phase ions. The reason is not entirely clear but may be due to electrochemical processes at the electrospray tip or solvent:silicate interactions.<sup>37</sup>

Adduct formation is also observed between neutral silicates and transition metal ions. Figure 2 shows the FT-ICR MS of a hexaquo nickelate in a dry acetonitrile solution of TEOS. The monoisotopic peak at 341.1371 Da can be assigned to the complex  $\text{Ni}(\text{Si}(\text{OEt})_4)_3$ . That stoichiometry results from complete replacement of the coordinated water molecules around the Ni(II) and suggests octahedral coordination. The suggestion that the silicon alkoxides bond to the nickel through the oxygen atoms in a bidentate fashion is consistent with the final coordination geometry of Ni(II) in processed silica xerogel glasses, suggesting that the Ni(II) acts as a template holding the silicates around

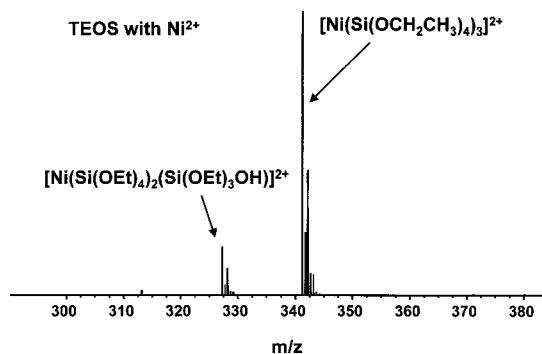


**Figure 2.** ESI FT-ICR positive-ion mass spectrum showing the ion types observed for alkoxy-silicates complexed with Ni(II) ions. The ion of 341.1371 Da is Ni(II) bound to three TEOS monomers. The ion of 327.1242 Da arises from hydrolysis of one of the alkoxy groups in the same complex.

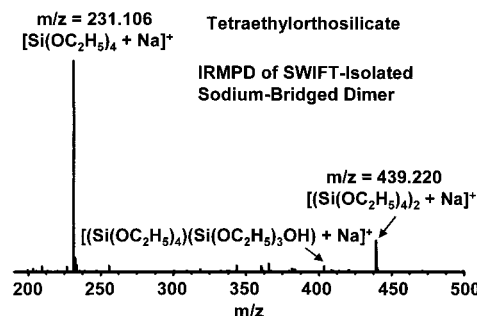


**Figure 3.** Infrared multiphoton dissociation (IRMPD) FT-ICR mass spectrum of electro-sprayed tetraethyl orthosilicate sodiated dimer. The parent ion was SWIFT-isolated and irradiated ( $10.6 \mu\text{m}$ ) at 4 W for 750 ms. The mass of the principal product ion confirms that its precursor is a sodium-bound dimer (see text).

it during hydrolysis and condensation.<sup>38</sup> A less abundant monoisotopic peak at  $327.1214 \pm 0.0004$  Da can be assigned to the hydrolysis product  $\text{Ni}(\text{Si}(\text{OEt})_4)_2(\text{Si}(\text{OEt})_3(\text{OH}))$  arising from reaction of the silicon with water displaced from the Ni(II) coordination sphere.

Although assignment of metal-complexed silicate species is relatively unambiguous based on accurate mass measurement alone, such assignments may be corroborated by tandem mass spectrometry. For example, infrared multiphoton dissociation (IRMPD) FT-ICR MS of the species at  $439.2152 \pm 0.0004$  Da produces primarily loss of a TEOS monomer (Figure 3), as expected for the sodium-bound dimer structure proposed in Figure 1. (The minor product corresponding to loss of  $\text{C}_2\text{H}_4$  may be interpreted as a McLafferty-like rearrangement.) Similar results have been seen previously for the protonated monomer of TEOS.<sup>39</sup> That the silicates themselves do not dissociate by IRMPD is readily explained. First, low-intensity IRMPD is expected to activate the lowest energy dissociation pathway.<sup>31,40</sup> Second, the high bond energy of Si-O ( $D_{298}^0 = 536$  kJ/mol, 5.6 eV from  $\text{HO}-\text{Si}(\text{CH}_3)_3$ ) vs the O-Na bond energy ( $D_{298}^0 = 256$  kJ/mol, 2.7 eV) makes dissociation of the complex the lower energy pathway.<sup>41</sup>

(36) Cotton, F. A.; Wilkinson, G. *Adv. Inorg. Chem.*, 4th ed.; John Wiley and Sons: New York, 1980; Vol. 1.

(37) Van Berkel, G. J. *The Electrolytic Nature of Electrospray*; Van Berkel, G. J., Ed.; John Wiley and Sons: New York, 1997; Vol. 1, pp 65–105.

(38) Sakka, S.; Ito, S.; Kamiya, K. *J. Non-Cryst. Solids* **1985**, *71*, 311.

(39) Olesik, S. V.; Kenny, V. D. *J. Am. Soc. Mass. Spectrom.* **1994**, *5*, 544–552.

(40) Dunbar, R. C. *J. Chem. Phys.* **1991**, *95*, 2537–2548.

(41) Lide, D. R. *CRC Handbook of Chemistry and Physics*; Lide, D. R., Ed.; CRC Press: Boca Raton, FL, 1999; Vol. 79, pp 9-51–9-53.



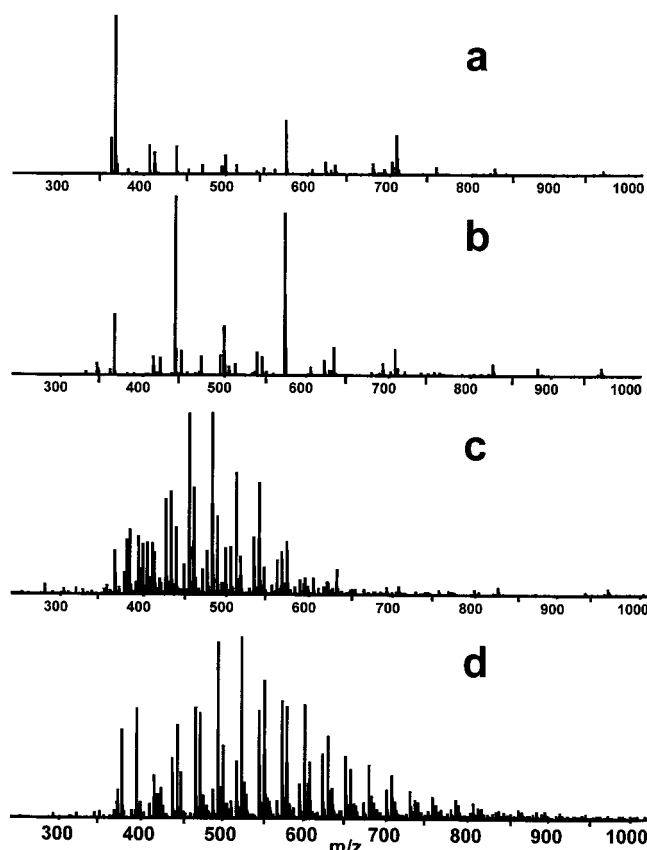


**Figure 4.** Time-resolved ESI FT-ICR positive-ion mass spectra of TEOS with added acid catalyst. Each spectrum results from a sample of TEOS reacting with water, dissolved in acetonitrile with sodium triflate added to promote cationization. (A) TEOS:H<sub>2</sub>O at a 1:4 mole ratio, prior to adding acetic acid. (B) Same sample, 5 min after addition of acetic acid (0.05 mol %). (C) As in (B), but after 6 h of reaction. (D) As in (B), but after 18 h of reaction.

**Silicate Speciation.** Alkali metal complexes are also formed from silicate species generated during the sol-gel process, rendering those products visible by ESI FT-ICR MS. Spectra collected at various stages of the time evolution of an aqueous/acetonitrile TEOS sol-gel solution (1:4, Si:H<sub>2</sub>O) are shown in Figure 4. Despite the very slow reactivity of TEOS with water in the absence of a catalyst, the FT-ICR mass spectrum taken after the addition of water (Figure 4a) shows a number of products, with dominant species at 365.1426, 573.2550, and 707.2978 Da, corresponding to [Si<sub>2</sub>O(OEt)<sub>6</sub> + Na]<sup>+</sup>, [Si<sub>2</sub>O(OEt)<sub>6</sub> + Si(OEt)<sub>4</sub> + Na]<sup>+</sup>, and [(Si<sub>2</sub>O(OEt)<sub>6</sub>)<sub>2</sub> + Na]<sup>+</sup>. Other species include hydrolyzed condensation products such as [Si<sub>2</sub>O(OEt)<sub>5</sub>OH + Na]<sup>+</sup>, [Si<sub>2</sub>O(OEt)<sub>5</sub>OH + Si(OEt)<sub>4</sub> + Na]<sup>+</sup>, and [Si<sub>2</sub>O(OEt)<sub>5</sub>OH + Si(OEt)<sub>4</sub> + Na]<sup>+</sup>. The mass spectrum acquired immediately (i.e., 5 min) after addition of acid (Figure 4b) shows an increase in species between 300 and 800 Da, with dominant species observed at 439.2152 and 573.2550 Da. As the reaction evolves, spectra taken at 6 and 18 h (Figures 4c and 4d) show a continuous increase in the number of species with a general shift in the centroid of the mass distribution envelope to higher molecular weight.

A strong advantage of the ESI FT-ICR MS technique is that species spanning a relatively broad molecular weight range can be observed simultaneously (in a second or so) and at each of the multiple stages of

hydrolysis. Figure 5 shows the mass region between 300 and 700 Da for an acid-catalyzed sol-gel collected 11 h after addition of the acid. All species are observed as sodium cation adducts and many are dimeric in the silicate species. For example, the peak at 448.8976 Da (see inset at upper left in Figure 5) is a sodium adduct containing both completely hydrolyzed di- and trisilicate oligomers. Also indicated in the spectrum are several of the partial hydrolysis products of the disilicate (appearing also as dimers bound to sodium at 439.2153 and 573.2550 Da). Although not explicitly shown, all other degrees of hydrolysis (i.e., replacement of 1, 2, 3, ..., ethoxy by hydroxyl groups) for the disilicate species can also be resolved. Finally, a completely alkoxyated tetrasilicate species is observed as a 1:1 adduct with sodium at 633.2220 Da. To the best of our knowledge, this characterization of oligomeric silicate species is the most complete to date. A list of the silicate and polysilicate species present at significantly above-threshold relative abundance in the mass spectrum of Figure 5 is given in Table 1. Despite the cation adduction needed to carry silicate species into the gas phase, thereby complicating the mass spectrum, the high mass resolving power and high mass accuracy of FT ICR MS permit the unambiguous assignment of a wide variety of species of different sizes and complexity.

**Electrospray Ionization Efficiency.** Although electrospray ionization efficiency can vary between different compounds, the yields are generally similar for sterically unhindered species in the same family (as in the present examples). For the related poly(dimethylsiloxane) polymers, ESI FT-ICR MS ionization efficiency has been shown to be independent of molecular weight.<sup>42</sup> An exception is that steric interactions can prevent ion formation. For example, we dissolved TEOS into 2-propanol (excess) and added acid catalysts to see if we could observe transesterification at the TEOS center. In fact, no transesterification products were observed, even though such species had previously been observed in solution by <sup>29</sup>Si NMR,<sup>43,44</sup> presumably because the transesterified products were too sterically hindered by the bulky isopropyl groups to allow for ion or dimer formation. Thus, highly branched species or those with large alkyl groups may be under-represented in the mass spectrum vs their relative abundance in solution.

**Concentration Range.** One of the strengths of ESI FT-ICR MS is that very high molecular weight species can be observed. In fact, we have observed silsequioxanes with molecular weights as high as 1.6 kDa by ESI FT-ICR MS. Nevertheless, for the present sol-gel system, the highest observed molecular weight is 933 Da, although we have observed species up to 1301 Da under other conditions (e.g., substoichiometric water, 1-month reaction time). We therefore attribute the absence of high-mass ions in the present experiments to their low absolute and/or relative concentration. First, note that the solutions are made up at concentrations typical of the sol-gel process but are diluted to 300 μM

(42) Yan, W.; Ammon, D. M. J.; Gardella, J. A. J.; Maziarz, E. P. I.; Hawkrige, A. M.; Grobe, G. L. I.; Wood, T. D. *Eur. Mass Spectrom.* **1998**, *4*, 467–475.

(43) Zerda, T. W.; Artaki, I.; Jonas, J. *J. Non-Cryst. Solids* **1986**, *81*, 365–379.

(44) Bernards, T. N. M.; Vanbommel, M. J.; Boonstra, A. H. *J. Non-Cryst. Solids* **1991**, *134*, 1–13.

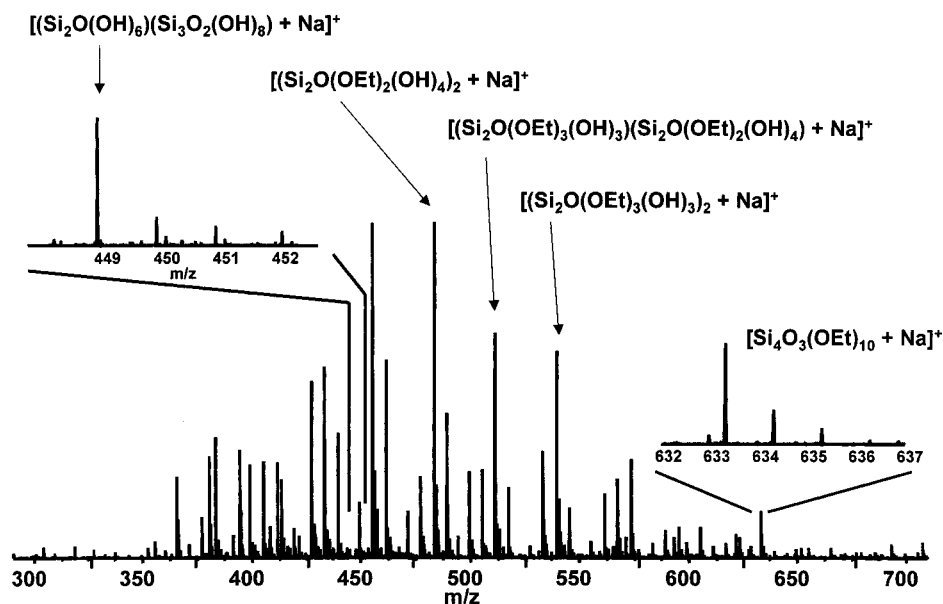


**Figure 5.** ESI FT-ICR positive-ion mass spectrum of TEOS reacted with water in a 1:4 mole ratio. This spectrum shows the complete hydrolysis series for the dimeric species, ranging from peralkylated to perhydroxylate silicate species.

**Table 1. Mass (in Dalton) and Chemical Formula Assignment for the Singly Charged Ions in the ESI FT-ICR Mass Spectrum Shown in Figure 3<sup>a</sup>**

measured mass (Da)	elemental composition
365.1423	$[(\text{Si}_2\text{O}(\text{OEt})_6 + \text{Na})^+]$
499.1831	$[(\text{Si}_3\text{O}_2(\text{OEt})_8 + \text{Na})^+]$
471.1513	$[(\text{Si}_3\text{O}_2(\text{OEt})_7\text{OH} + \text{Na})^+]$
443.1203	$[(\text{Si}_3\text{O}_2(\text{OEt})_6(\text{OH})_2 + \text{Na})^+]$
415.0883	$[(\text{Si}_3\text{O}_2(\text{OEt})_5(\text{OH})_3 + \text{Na})^+]$
633.2220	$[(\text{Si}_4\text{O}_3(\text{OEt})_{10} + \text{Na})^+]$
605.1926	$[(\text{Si}_4\text{O}_3(\text{OEt})_9\text{OH} + \text{Na})^+]$
577.1611	$[(\text{Si}_4\text{O}_3(\text{OEt})_8(\text{OH})_2 + \text{Na})^+]$
549.1288	$[(\text{Si}_4\text{O}_3(\text{OEt})_7(\text{OH})_3 + \text{Na})^+]$
707.2978	$[(\text{Si}_2\text{O}(\text{OEt})_6)_2 + \text{Na})^+]$
679.2629	$[(\text{Si}_2\text{O}(\text{OEt})_6 + \text{Si}_2\text{O}(\text{OEt})_5\text{OH}) + \text{Na})^+]$
651.2341	$[(\text{Si}_2\text{O}(\text{OEt})_5(\text{OH})_2 + \text{Na})^+]$
623.2024	$[(\text{Si}_2\text{O}(\text{OEt})_4(\text{OH})_2 + \text{Si}_2\text{O}(\text{OEt})_5\text{OH}) + \text{Na})^+]$
595.1719	$[(\text{Si}_2\text{O}(\text{OEt})_4(\text{OH})_2)_2 + \text{Na})^+]$
567.1403	$[(\text{Si}_2\text{O}(\text{OEt})_3(\text{OH})_3 + \text{Si}_2\text{O}(\text{OEt})_4(\text{OH})_2) + \text{Na})^+]$
539.1077	$[(\text{Si}_2\text{O}(\text{OEt})_3(\text{OH})_3)_2 + \text{Na})^+]$
511.0763	$[(\text{Si}_2\text{O}(\text{OEt})_2(\text{OH})_4 + \text{Si}_2\text{O}(\text{OEt})_3(\text{OH})_3) + \text{Na})^+]$
483.0450	$[(\text{Si}_2\text{O}(\text{OEt})_2(\text{OH})_4)_2 + \text{Na})^+]$
455.0131	$[(\text{Si}_2\text{O}(\text{OEt})_1(\text{OH})_5 + \text{Si}_2\text{O}(\text{OEt})_2(\text{OH})_4) + \text{Na})^+]$
426.9821	$[(\text{Si}_2\text{O}(\text{OEt})_1(\text{OH})_5)_2 + \text{Na})^+]$
398.9506	$[(\text{Si}_2\text{O}(\text{OH})_6 + \text{Si}_2\text{O}(\text{OEt})_1(\text{OH})_5) + \text{Na})^+]$
370.9203	$[(\text{Si}_2\text{O}(\text{OH})_6)_2 + \text{Na})^+]$
617.0858	$[(\text{Si}_2\text{O}(\text{OEt})_6 + \text{Si}_2\text{O}_3(\text{OH})_8) + \text{Na})^+]$
589.0529	$[(\text{Si}_2\text{O}(\text{OEt})_5\text{OH} + \text{Si}_2\text{O}_3(\text{OH})_8) + \text{Na})^+]$
561.0226	$[(\text{Si}_2\text{O}(\text{OEt})_4(\text{OH})_2 + \text{Si}_2\text{O}_3(\text{OH})_8) + \text{Na})^+]$
532.9913	$[(\text{Si}_2\text{O}(\text{OEt})_3(\text{OH})_3 + \text{Si}_2\text{O}_3(\text{OH})_8) + \text{Na})^+]$
504.9897	$[(\text{Si}_2\text{O}(\text{OEt})_2(\text{OH})_4 + \text{Si}_2\text{O}_3(\text{OH})_8) + \text{Na})^+]$
476.9292	$[(\text{Si}_2\text{O}(\text{OEt})_1(\text{OH})_5 + \text{Si}_2\text{O}_3(\text{OH})_8) + \text{Na})^+]$
448.8976	$[(\text{Si}_2\text{O}(\text{OH})_6 + \text{Si}_2\text{O}_3(\text{OH})_8) + \text{Na})^+]$

<sup>a</sup> Mass accuracy is  $\sim 1$  ppm, based on internal calibration (see text). The elemental composition of each proposed sodium-bound dimer is represented according to its constituent monomers.

for electrospraying. Second, FT-ICR MS has a potential dynamic range of 3–4 orders of magnitude in a single spectrum, expandable by another several orders of magnitude by acquisition of a second spectrum from which the most abundant species have been removed by mass-selective ion ejection.<sup>45</sup> Thus, for the present

experiments, we expect to observe species from 300 nM to 300  $\mu\text{M}$  concentration in a given mass spectrum. Condensation of the silicates into progressively higher molecular weight species is necessarily accompanied by a concomitant decrease in concentration that may ultimately drop below detectability. Thus, the maximum observable molecular weight will be dictated by the extent of reaction and the molecular weight distribution for a given set of reaction conditions.

**Linearity of ESI FT-ICR MS Signal with Solution-Phase Concentration.** To provide useful insights into molecular growth pathways in sol–gel or other inorganic polymerization processes, it is necessary to quantify the relative amounts of the observed species. For the related poly(dimethylsiloxane) polymers, the ESI FT-ICR mass spectral peak area has been shown to vary linearly with solution concentration over about 2 orders of magnitude.<sup>42</sup> Similarly, the FT-ICR MS peak area for electrosprayed cyclosporin is linear in concentration from 5 to 250 ng/mL.<sup>46</sup>

## Conclusions

We have successfully obtained electrospray ionization FT-ICR mass spectra of complex silicate and polysilicate species generated in the sol–gel process. Electrospray ionization renders these species observable in the gas phase at concentrations suitable for mass spectral analysis by virtue of their tendency to form strong complexes with both alkali metal and transition metal cations. Thus, association processes in the sol–gel solution may be more important than previously thought. Although a specific silicate species structure cannot be inferred from mass alone (e.g., branched and unbranched isomers have the same mass), interrogation can be carried out by tandem mass spectrometry as for the  $[(\text{Si}(\text{OCH}_2\text{HC}_3)_4)_2 + \text{Na})^+]$  ions. ESI coupled with FT-ICR MS thus constitutes a potentially powerful tool for the elucidation of molecular species and growth path-

(45) Wang, T.-C. L.; Ricca, T. L.; Marshall, A. G. *Anal. Chem.* **1986**, *58*, 2935–2938.

(46) Gordon, E. F.; Muddiman, D. C. *Rapid Commun. Mass Spectrom.* **1999**, *13*, 164–171.

ways in sol-gel and other inorganic-materials-forming reactions.

**Acknowledgment.** We thank John P. Quinn of the National High Magnetic Field Laboratory for technical assistance. This work was supported by the NSF (DMR-

96-23570 and CHE-93-22824) and the NSF National High Field FT-ICR Facility (CHE-94-13008 and CHE 99-09502), Florida State University, and the National High Magnetic Field Laboratory in Tallahassee, FL.

CM000934M